BİNGÖL ÜNİVERSİTESİ
TEKNİK BİLİMLER DERGİSİ

Bingöl Üniversitesi Teknik Bilimler Dergisi
Bingol University Journal of Technical Science
e-ISSN: 2757-6884

Cilt:6, Sayı: 2, Sayfa: 51-63, 2025
Araştırma Makalesi

Volume:6, Number:2, Page: 51-63, 2025
Research Article

Doi: 10.5281/zenodo.17839127

Experimental Investigation of Optical Pulse Generation in Two-Section and Three-Section Diode Lasers with Different Configuration

Rukiye AKSAKAL [1]*, Bülent ÇAKMAK [2]

[1] Erzurum Technical University, Department of Electrical and Electronic Engineering, Erzurum, Türkiye
ORCID: 0000-0002-2708-2937, E-mail: rukiye.aksakal@erzurum.edu.tr

[2] Erzurum Technical University, Department of Electrical and Electronic Engineering, Erzurum, Türkiye
ORCID: 0000-0002-9939-4809, E-mail: bulent.cakmak@erzurum.edu.tr

(Alınış/Arrival: 20.05.2025, Kabul/Acceptance: 28.05.2025, Yayınlanma/Published: 15.12.2025)

Abstract
In this study, optical pulses measurements obtained from two-section and three-section InGaAsP/InP diode lasers operating at a wavelength of 1350 nm are presented, with the cavity length kept constant at 315 µm, while the positions of the gain and absorber sections are varied. A 2 kHz signal with a 100 µs pulse width was applied to the gain sections along with a 20 mA DC current, while a reverse bias voltage ranging from 0 to -1.5 V was applied to the absorber section. The current applied to the gain section and the reverse bias voltage applied to the absorber section were kept constant at certain values for both laser types, and the resulting pulse amplitudes and durations were analyzed. The pulses obtained from the three-section lasers, where the absorber section was positioned in the middle (between the two gain sections), exhibited higher amplitudes than those obtained from the two-section lasers, and their pulse widths were approximately 5% narrower. In contrast, lasers with the absorber at the end produced higher output power compared to single-gain lasers, but wider pulse widths were obtained than lasers with the absorber at the middle.

Keywords: *Laser*, Multisection, *Optical pulse generation*, Semiconductor, *InGaAsP/InP Diode Lasers*

Farklı Konfigürasyona Sahip İki Bölümlü ve Üç Bölümlü Diyot Lazerlerde Optik Darbe Üretiminin Deneysel İncelenmesi

Özet
Bu çalışmada, 1350 nm dalga boyunda çalışan iki ve üç kesitli InGaAsP/InP diyot lazerlerinden elde edilen optik darbe ölçümleri, kavite uzunluğu 315 µm'de sabit tutulurken, kazanç ve soğurucu bölümlerin konumları değiştirilerek sunulmuştur. 100 µs darbe genişliğine sahip 2 kHz'lik bir sinyal, 20 mA DC akımla birlikte kazanç bölümlerine uygulanırken, soğurucu bölüme 0 ile -1,5 V arasında değişen bir ters kutuplu gerilim uygulanmıştır. Kazanç bölümüne uygulanan akım ve soğurucu bölüme uygulanan ters kutuplu gerilim her iki lazer tipi için de belirli değerlerde sabit tutulmuş ve ortaya çıkan darbe genlikleri ve süreleri analiz edilmiştir. Soğurucu bölümün ortada (iki kazanç bölümü arasında) konumlandırıldığı üç kesitli lazerlerden elde edilen darbeler, iki kesitli lazerlerden elde edilenlerden daha yüksek genlikler sergilemiş ve darbe genişlikleri yaklaşık %5 daha dar olmuştur. Buna karşılık, soğurucu bölümü uçta olan

lazerler, tek kazançlı lazerlere kıyasla daha yüksek çıkış gücü ürettiler, ancak darbe genişlikleri, soğurucu bölümü ortada olan lazerlere göre daha geniş elde edilmiştir.

Keywords: *Lazer,* Çok bölümlü, *Optik darbe üretimi*, Yarı iletken, *InGaAsP/InP diyot lazer*

1. INTRODUCTION

The rapid advancement of optical communication technologies has been significantly influenced by the development of semiconductor lasers. Since their first demonstration in 1962, these lasers have enabled substantial progress in the realization of high-speed, energy-efficient communication systems [1]. With the continuous increase in global information traffic, the demand for faster and more efficient optical communication solutions has intensified. To meet this demand, semiconductor lasers capable of operating at high speeds with low threshold currents and minimal cooling requirements are essential, offering cost-effective and energy-efficient alternatives[2].

InP-based heterostructures have demonstrated remarkable potential for various applications, including low-loss fiber-optic communications, integrated photonics, optical switching and free-space communications [1-3]. Among the widely employed techniques for generating ultrashort optical pulses, mode-locking, Q-switching, and gain-switching have proven to be effective in semiconductor lasers. Mode-locked lasers are particularly well-suited for generating the shortest optical pulses with minimal timing jitter. However, their pulse energies are generally lower, and their repetition rate is predominantly determined by the cavity length. In contrast, Q-switching enables the generation of high peak-power pulses, often achieved by incorporating a saturable absorber within the laser cavity to enhance output power[4]. Gain-switching offers flexibility in repetition rate and eliminates the need for complex cavity structures, making it attractive for certain applications. However, its peak power output is generally limited, particularly in the longer wavelength regions (1350–1550 nm)[5]. Among these techniques, Q-switching remains one of the most effective processes for generating high peak-power pulses in semiconductor lasers, with the saturable absorber section playing a crucial role in power enhancement[6]. One of the promising approaches to further enhance pulse power in semiconductor lasers is the use of tapered waveguides. This technique has been successfully implemented in various laser types, including mode-locked [7,8], gain-switched[9], and Q-switched lasers[10,11]. By linearly expanding the waveguide from a transversely monomode structure, a well-defined low-order optical mode is formed, which propagates into a broader gain region. This waveguide geometry effectively mitigates the detrimental effects of gain saturation and catastrophic optical damage by distributing the optical mode over a larger cross-section, particularly near the laser facets[12].

In the 1.5 μm wavelength range, InGaAsP-based diode lasers have exhibited significant advancements in pulse energy and duration. These lasers have achieved pulse energies of up to 94 pJ with durations as short as 750 ps, making them highly suitable for telecommunications and high-speed data processing applications [13]. Recent developments in mode-locking and Q-switching techniques have further enhanced the capabilities of semiconductor lasers, enabling the generation of optical pulses with peak powers reaching several watts [14].

Cavity length plays a critical role in ultrashort pulse generation in semiconductor lasers. A reduction in cavity length leads to an increase in both repetition rate and pulse frequency [13-15]. However, semiconductor lasers incorporating two gain sections have been shown to produce shorter pulse durations and higher output power compared to their single-gain-section

counterparts [16-19). Previous studies have primarily focused on semiconductor lasers with single and dual gain sections, alongside an absorption section, typically featuring cavity lengths exceeding 500 μm [19-22]. As cavity length increases, a higher injection current is required for the gain region and a higher reverse bias voltage is necessary for the absorption region to achieve effective mode-locking [21]. Although the generation of short optical pulses using multi-section semiconductor lasers with mode-locking and Q-switching techniques has been widely investigated in the literature, the majority of these studies have focused on cavity lengths exceeding 500 μm and fixed absorber positions. Especially in the design of compact structures that can operate at low current and voltage levels, the influence of absorber placement in cavities shorter than 350 μm has not been thoroughly examined. In this study, the cavity length was reduced to 315 μm, and InGaAsP/InP lasers with two and three sections were fabricated with the absorber region positioned either in the middle (between two gain sections) or at the end. The effects of these different configurations on pulse width and output power were experimentally investigated under identical driving conditions. In this respect, the study differs from conventional approaches in the literature by presenting a comparative analysis of absorber location in ultra-compact cavity structures, offering original insights for the design of compact, short-pulse semiconductor lasers.

In this study, the effects of different structural configurations on optical pulse generation in two-section and three-section semiconductor lasers are experimentally investigated. Particular attention is given to the influence of cavity length, waveguide design, and etching parameters on pulse characteristics. The position of the absorber section within the laser structure is considered a critical factor affecting key parameters such as pulse amplitude, duration, and output power. The current applied to the gain section and the reverse bias voltage applied to the absorber section were kept constant across all configurations. The results demonstrate that three-section lasers, especially those with the absorber section placed in the middle, exhibit superior performance with higher pulse amplitudes and narrower pulse widths compared to two-section lasers. This study provides valuable insights for designing high-performance semiconductor lasers capable of generating ultrashort pulses, which are essential for applications in optical communication and high-speed data processing.

2. DESIGN AND FABRICATION OF THE LASERS

The two-section and three-section lasers were fabricated with cavity lengths kept below 500 μm. Undoped InP substrates were used, grown by metal organic chemical vapor deposition (MOCVD). Standard photolithography was employed to pattern the samples, creating an etch mask with resist patterns on 200 nm and 50 nm thick sputter-deposited Si_3N_4 and Ni layers. The mask design included waveguides with lengths of 9 μm and 12 μm. The mask pattern was transferred to the substrate using reactive ion etching (RIE) with CHF_3, followed by O_2 plasma treatment to remove the photoresist. Ridge waveguides were then formed by inductively coupled plasma reactive ion etching (ICP-RIE), with varied etching depths to refine the structure. By modifying etching parameters such as gas mixtures, process conditions, and mask materials, it was possible to control the trade-off between etching rate and anisotropy.

The photolithography process created an etching mask consisting of Si_3N_4 and thermally evaporated Ni layers, deposited via Plasma-Enhanced Chemical Vapor Deposition (PECVD), with respective thicknesses of 200 nm and 50 nm. The mask pattern was transferred to the substrate through ICP-RIE using a $CH_4/H_2/Cl_2$ gas mixture (10/20/6 sccm). The etching process was carried out without substrate heating, with the ICP power set to 400 W and the RF power maintained at 150 W, at a process pressure of 2 Pa. The etching continued until the etch-stop

layer was reached, achieving a depth of approximately 1.5 µm for InGaAsP/InP. The two-layer mask (Ni/Si_3N_4) was removed using H_2SO_4 and HF, respectively. The etching quality was thoroughly analyzed using scanning electron microscopy (SEM), optical microscopy, and 3D profilometry. Depending on the gas mixture used, an average surface roughness (Ra) of 0.137 µm and an anisotropic profile of approximately 90° were achieved. These results demonstrate the high quality of the etching process and the reproducibility of our fabrication method. Based on the optical output measurements, the slope efficiency of the device was calculated to be approximately 0.3 µW/mA within the linear operating region. This value reflects the rate at which the optical power increases with the injection current and indicates consistent light output performance under the given operating conditions. The simplified schematic of the InGaAsP/InP material structure is given in Figure 1.

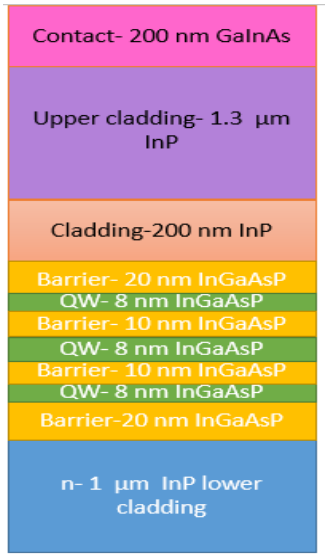

Figure 1. Basic cross-sectional schematic of the material structure

The InGaAsP/InP (1330 nm) material structure comprises the following layers, starting from the InP substrate and including two QWs: a 1 µm thick n-type InP lower cladding layer, an undoped 524 nm thick waveguide layer, a 0.2 µm thick p-type InP transition layer, a 80 nm thick p-type InGaAsP etch-stop layer, a 1.3 µm thick p-type InP upper cladding layer, and a 200 nm thick p-type InGaAs contact layer. The active region within the waveguide consists of two 8 nm thick InGaAsP QWs surrounded by three 10 nm thick InGaAsP barriers. These barriers are further enclosed within a discrete confinement heterostructure layer composed of a 0.22 µm thick InGaAsP quaternary compound.

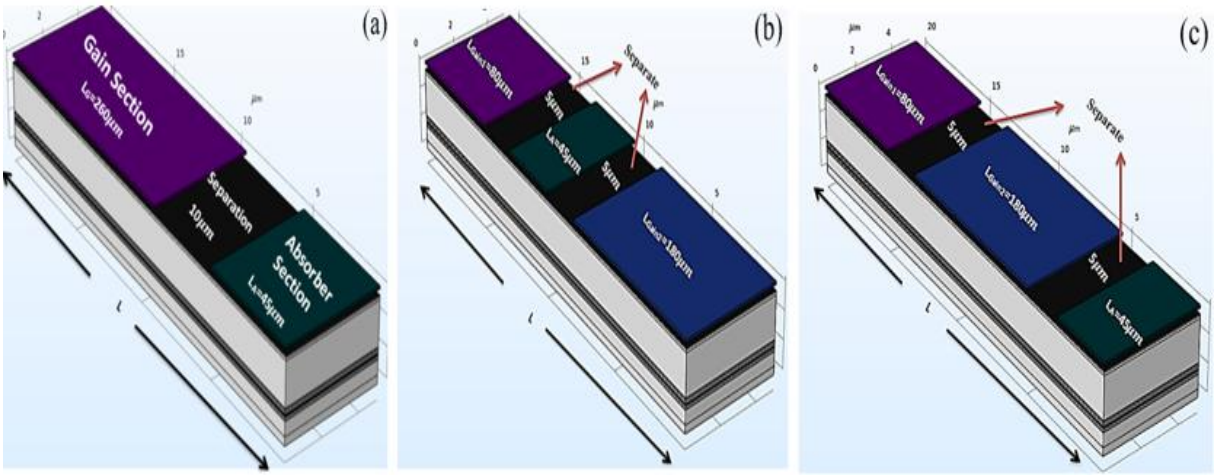

Figure 2. Various designs of semiconductor lasers used in the fabrication: (a) L_G= 260 μm, two-section laser (one gain and one absorber section); (b) L_{G1}= 80 μm, L_{G2}= 180 μm, three-section laser (two gain and one absorber sections); and (c) Absorber section at the end: L_{G1}= 80 μm, L_{G2}= 180 μm (two gain and one absorber sections), with L_A = 45 μm for all.

Schematic structures of the lasers studied experimentally are shown in Figure 2 [22]. In Figure 2 (a), a two-section laser with a one gain section is shown (L_{gain}= 260 μm and L_A= 45 μm); in Figure 2 (b), a three-section laser with two gain regions and the absorber region in the middle is presented (L_{gain1}= 80 μm, L_{gain2}= 180 μm and L_A= 45 μm); and in Figure 2 (c), a three-section laser with two gain regions and the absorber region at the end (L_{gain1}= 80 μm, L_{gain2}= 180 μm and L_A= 45 μm) is shown. The total cavity length has been fixed at 315 μm.

The experimental setup used for optical pulse characterization is schematically illustrated in Figure 3. This setup includes the laser under test, current and voltage sources for driving the gain and absorber sections, and a high-speed photodetector connected to an oscilloscope for time-domain pulse measurements. The configuration allows precise control of the bias conditions and enables accurate observation of pulse characteristics such as amplitude and duration under different laser structures.

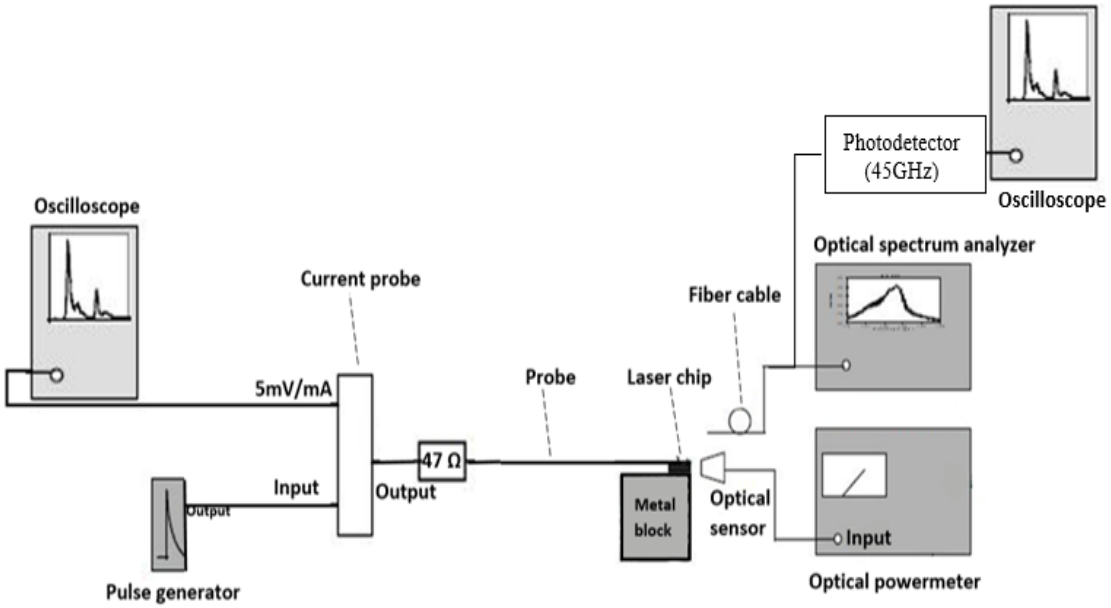

Figure 3. *Schematic block diagram of the experimental setup used for optical pulse characterization.*

3. EXPERIMENTAL RESULTS

3.1 The Optical Pulses Obtained From The Two-Section Lasers

In the two-section lasers, a 2 kHz signal with a pulse width of 100 μs was applied to the gain region with a 20 mA DC current, while a reverse bias voltage was applied to the absorber region. The fiber cable was connected to the photodetector, and the photodetector output was connected to the instrumentation amplifier's input. The output of the amplifier was then connected to the oscilloscope to observe the optical pulses (Figure 4). Optical pulses were obtained for reverse bias voltages of -0.5 V, -1 V, and -1.5 V. As shown in Figures 4 (a) and (b), when the reverse bias voltage was reduced from -0.5 V to -1 V, the output power decreased, and the pulse width dropped from 11.6 ns to 10.8 ns. When the reverse bias voltage was reduced to -1.5 V, the pulse amplitude decreased, and the pulses were observed to be distorted. The repetition rate of the pulses was obtained to be 28 MHz.

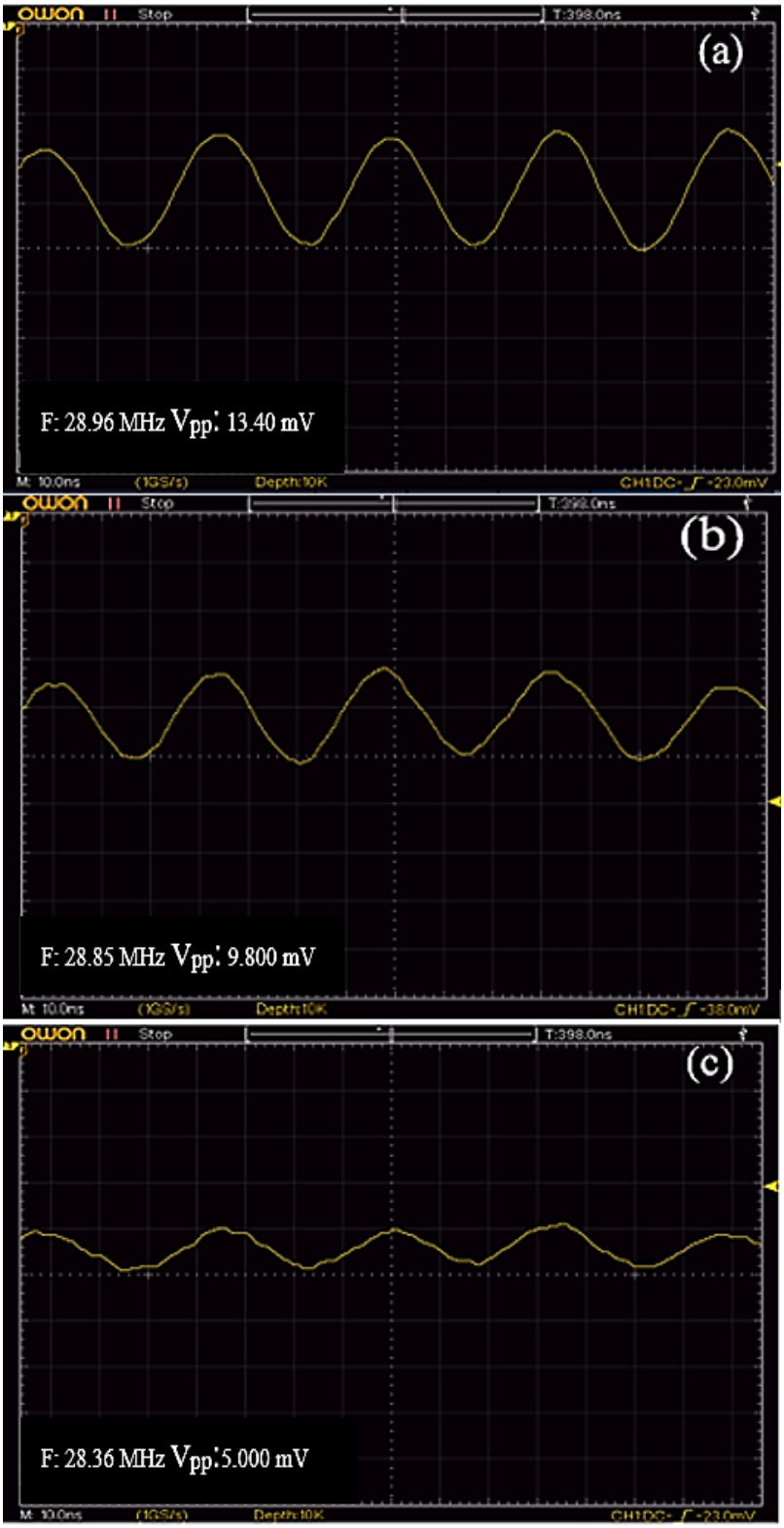

Figure 4. *Optical pulses obtained from two-section (single gain and absorber) InGaAsP/InP diode lasers under different reverse bias voltages: (a) V = -0.5 V, (b) V = -1 V, and (c) V = -1.5 V. The gain section was driven with a 2 kHz signal (100 µs pulse width) and a 20 mA DC current.*

3.2 The Optical Pulses Obtained From The Three-Section Lasers

In the three-section lasers (with two gain regions and the absorber region in the middle), a 2 kHz signal with a pulse width of 100 µs was applied to the gain sections, along with a 20 mA

DC current, while a reverse bias voltage was applied to the absorption region. As the applied reverse bias voltage was reduced from -0.5 V to -1.5 V, the optical pulses obtained are shown in Figure 5. When V = -0.5 V (Figure 5 (a)), the pulse width was obtained to be 11.2 ns, whereas at V = -1.5 V, the pulse width decreased to 10.2 ns, as shown in Figure 5 (c). In addition, the output power also decreased. The repetition rate of the pulses was between 27-28 MHz.

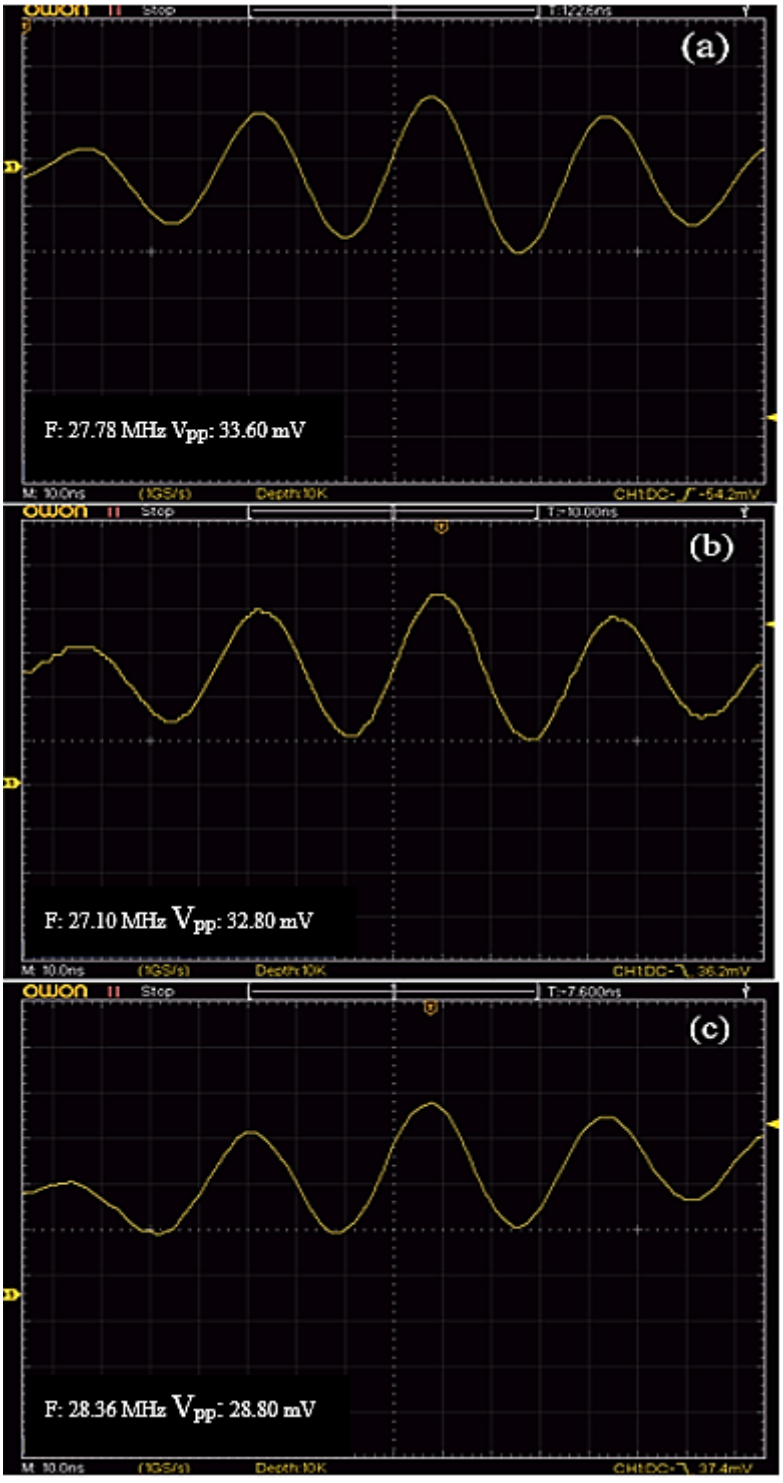

Figure 5. *Optical pulses obtained from three-section InGaAsP/InP diode lasers (with two gain regions and the absorber region in the middle) under different reverse bias voltages: (a) V = -0.5 V, (b) V = -1 V, and (c) V = -1.5 V. The gain sections were driven with a 2 kHz signal (100 µs pulse width) and 20 mA DC current.*

The optical pulses obtained from the three-section lasers (comprising two gain regions and a terminal absorber region) are shown in Figure 6. These pulses were generated when a 20 mA DC current, combined with a 2 kHz signal having a pulse width of 100 µs, was applied to the gain sections, and a reverse bias voltage was applied to the absorption region. As the applied reverse bias voltage decreased, the pulse amplitude decreased as well, but it was still higher compared to the single gain section lasers. Furthermore, the pulse width of 10.6 ns was longer than that of the lasers with the absorber section in the middle (τ = 10.2 ns).

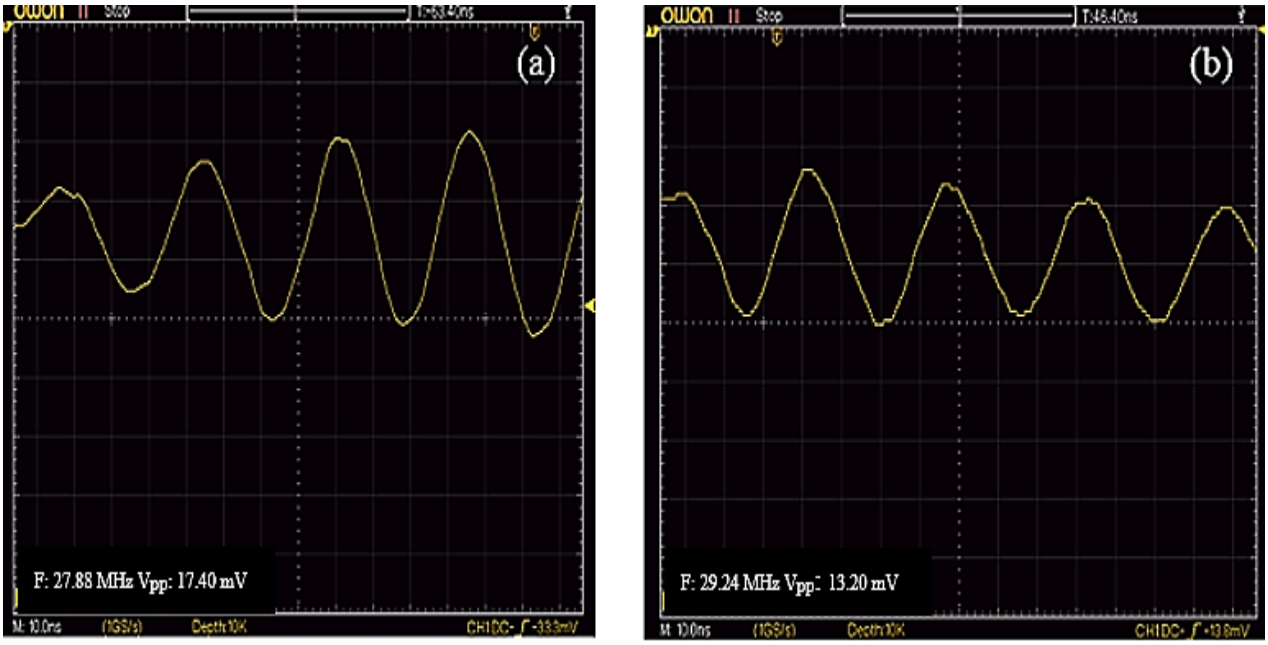

Figure 6. *Optical pulses obtained from three-section InGaAsP/InP diode lasers (two gain regions with the absorber region at the end) under different reverse bias voltages: (a) V = -0.5 V and (b) V = -1.5 V. The gain sections were driven with a 2 kHz signal (100 µs pulse width) and 20 mA DC current.*

Table 1. Optical pulse characteristics obtained from different laser structures under various reverse bias voltages.

Laser Structure	Reverse Bias (V)	Frequency (MHz)	Peak Voltage (Vpp)	Pulse width (ns)
Two-section (1 gain section + 1 absorber section)	-0.5	28.94	13.40 mV	11.6
	-1.0	28.85	9.80 mV	
	-1.5	28.36	5.00 mV	10.8
Three-section (2 gain sections + central absorber section)	-0.5	27.78	33.60 mV	11.2
	-1.0	27.10	32.80 mV	
	-1.5	28.36	28.80 mV	10.2
Three-section (2 gain sections + absorber section at the end)	-0.5	27.88	17.40 mV	
	-1.5	29.24	13.20 mV	10.6

Figures 4, 5, and 6 respectively present the optical pulses obtained at various reverse bias voltages from different laser configurations: Figure 4 shows pulses from two-section lasers with one gain section and one absorber section; Figure 5 depicts pulses from three-section lasers with two gain sections and a centrally positioned absorber; and Figure 6 illustrates pulses from three-section lasers with two gain sections and an absorber positioned at the end. As shown, while maintaining a constant cavity length, the positions of gain and absorber sections were varied under consistent operating conditions. Comparative analysis of the optical pulses reveals distinct pulse characteristics for each configuration as a function of reverse bias voltage. In the two-section laser, decreasing the bias from -0.5 V to -1.5 V reduced the pulse width from 11.6

ns to 10.8 ns with a repetition rate of 28 MHz; however, higher bias voltages led to pulse distortion and weakening. In the three-section laser with a central absorber, the pulse width decreased more significantly, from 11.2 ns to 10.2 ns, with repetition rates remaining between 27–28 MHz, indicating better pulse confinement. This corresponds to approximately a 5% reduction in pulse width compared to the two-section laser under similar bias conditions. In contrast, the three-section laser with the absorber at the end generated pulses with higher amplitudes than the two-section design, but with a slightly longer pulse width of 10.6 ns compared to the central absorber configuration. These results highlight the critical role of absorber positioning in optimizing pulse performance, demonstrating that three-section lasers with a central absorber provide both higher pulse amplitudes and shorter pulse durations. The comparative numerical data for reverse bias voltages, pulse frequencies, peak voltages, and pulse widths of the different laser structures are summarized in Table 1.

4. CONCLUSION

In this study, optical pulse generation from two-section and three-section InGaAsP/InP diode lasers operating at 1350 nm was investigated. The cavity length was kept constant while varying the positions of the gain and absorber sections. Both laser types were driven with a 2 kHz signal of 100 μs pulse width, applying a 20 mA DC current to the gain sections and reverse bias voltages ranging from 0 to -1.5 V to the absorber section. The oscilloscope traces and experimental data summarized in Table 1 demonstrate variations in pulse characteristics, such as pulse width and amplitude, depending on the laser structure and applied bias voltages. Notably, three-section lasers with the absorber positioned between two gain sections exhibited approximately 5% narrower pulse widths (10.2 ns for the three-section laser compared to 10.8 ns for the two-section laser at a reverse bias voltage of -1.5 V) and higher pulse amplitudes under similar bias conditions. The repetition rate remained stable within the 27–28 MHz range. Conversely, three-section lasers with the absorber at the cavity end generated pulses with higher amplitude than two-section lasers but slightly longer pulse widths (10.6 ns). These findings emphasize the critical role of absorber positioning in laser performance, influencing both pulse compression and amplitude enhancement. Future work will focus on exploring novel cavity designs and integrating avalanche current sources with these engineered cavities to achieve optical pulses with higher power and shorter durations. Additionally, integrating these devices into practical photonic and communication systems, along with durability and reliability testing, will be important avenues for research. Finally, the 1350 nm wavelength, corresponding to the low-loss transmission window in fiber optic communication, underscores the significant potential of these laser structures to improve performance in modern communication systems. The presented results provide a valuable foundation for developing compact and efficient semiconductor laser sources.”

Acknowledgements

The authors acknowledge the support of TUBITAK through project number 122E681 and the TUBITAK 2211C National PhD Scholarship Program provided by the Directorate of Science Fellowships and Grant Programs (BIDEB).

Ethical Statement

All procedures followed were in accordance with the ethical standards.

Conflict of Interest

There is no conflict of interest for conducting the research and/or for the preparation of the article.

Funding Statement

This study is supported by TUBITAK through project number 122E681 and the TUBITAK 2211C National PhD Scholarship Program, provided by the Directorate of Science Fellowships and Grant Programs (BIDEB).

Author Contributions

Rukiye Aksakal contributed to the writing of the original draft, editing, conceptualization, and conducting the experimental study. Bülent Çakmak contributed to the supervision and validation of the study, as well as the review and editing of the manuscript.

Data Availability Declaration

The authors confirm that all data generated or analysed during this study are included in this article.

REFERENCES

[1] Hall N, Fenner G H, Kingsley J D, Soltys T J, Carlson R D. Coherent light emission from GaAs. Physical Review Letters. 1962;9(1), 62–64.

[2] Nakamura T, Okuda T, Kobayashi R, Muroya Y, Tsuruoka K, Ohsawa Y, Tsukuda T, Ishikawa S. 1.3 μm AlGaInAs strain-compensated MQW-buried-heterostructure lasers for uncooled 10 Gb/s operation. IEEE Journal of Selected Topics in Quantum Electronics. 2005;11(1), 141–148.

[3] Cakmak B, Biber M, Karacali T, Duman C. A comparative study of fabrication of long wavelength diode lasers using CCl_2F_2/O_2 and H_2/CH_4. Optics and Photonics Journal. 2013;3(1), 21–24.

[4] Pilny R H, Döpke B, Brenner C, Klehr A, Knigge A, Tränkle G, Hofmann M R. Self-optimizing passively, actively and hybridly mode-locked diode lasers. CLEO/Europe EQEC Conference Proceedings. 2017.

[5] Stolarz P M, Javaloyes J, Mezosi G, Hou L, Ironside C N, Sorel M, Bryce A C, Balle S. Spectral dynamical behaviour in passively mode-locked semiconductor lasers. IEEE Photonics Journal. 2011;3(6), 1067–1082.

[6] Keller U. Recent developments in compact ultrafast lasers. Nature. 2003;424, 831–838.

[7] Schelte C, Gurevich S V, Javaloyes J. A functional mapping for passively mode-locked semiconductor lasers. Optics Letters. 2018;43, 2535–2538.

[8] Ma Y, Zhu X, Yang L, Tong M, Norwood R A, Wei H, Chu Y, Li H, Dai N, Peng J, Li J, Peyghambarian N. Numerical investigation of GHz repetition rate fundamentally mode-locked all-fiber lasers. Optics Express. 2019;27(10), 14487–14504.

[9] Duman C, Cakmak B. Time domain dynamic analysis of a 1550 nm monolithic two section mode-locked MQW laser. East Anatolian Science. 2015;2, 70–76.

[10] Adams M J, Steventon A G, Delvin W J, Henning I D. Semiconductor lasers for long-wavelength optical-fiber communications systems. Short Run Press Ltd. 1987.

[11] Zhang L M, Yu S F, Nowell M C, Marcenac D D, Carroll J E, Plumb R G S. Dynamic analysis of radiation and side-mode suppression in a second-order DFB laser using time-domain large-signal traveling wave model. IEEE Journal of Quantum Electronics. 1994;30, 1389–1395.

[12] Avrutin E A, Marsh J H, Portnoi E L. Monolithic and multi-gigahertz mode-locked semiconductor lasers: constructions, experiments, models, and applications. IEEE Proceedings of OptoElectronics. 2000;147, 251–278.

[13] Schwarz S, Baumgartner O, Austerer M, Andrews A M, Detz H, Strasser G. Ultrafast dynamics of monolithic semiconductor mode-locked lasers. Journal of Applied Physics. 2013;113, 083102.

[14] Thompson M G, Williams K A, White I H. High-performance ultrashort pulse generation using mode-locked quantum-dot semiconductor lasers. IEEE Journal of Quantum Electronics. 2006;42, 1032–1038.

[15] Martini R, Hofstetter D, Faist J, Sivco D L, Baillargeon J N, Cho A Y, Capasso F. High-frequency modulation with picosecond pulses in quantum cascade lasers. Electronics Letters. 2002;38, 181–182.

[16] Rafailov E U, Bimberg D, Avrutin E A. Quantum-dot mode-locked lasers and their applications: Review. Journal of Optics and Quantum Electronics. 2007;39, 973–1002.

[17] Liu X, Ling J, Yoo S, Shieh W. High-speed optical communication using mode-locked semiconductor lasers. Optics Express. 2010;18, 14632–14637.

[18] Wang C, Liu Y, Zhao H, Zhang Z, Xu J, Wang J. High-power passively mode locked semiconductor laser at 1550 nm. IEEE Photonics Technology Letters. 2012;24, 1706–1709.

[19] Schires K, Grillot F, Poingt F, Lhuillier J, Llopis O, Thevenin J. Repetition rate enhancement of a passively mode-locked quantum dash semiconductor laser using an external fibered feedback loop. Optics Express. 2013;21, 8894–8899.

[20] Duan L, Lu X, Yu J, Luo Y, Liu Y, Zhou H. Passive mode-locking of a two-section InGaAsP/InP quantum well laser at 1.55 μm. Optics Communications. 2015;356, 517–522.

[21] Pan S, Yang H, Wang F, Xu S, Chen H. Dynamic characteristics of a two-section passively mode-locked semiconductor laser with varied absorber length. Optics Express. 2016;24, 21484–21492.

[22] Aksakal R, Duman C, Cakmak B. Numerical investigation of 1550 nm passively mode-locked diode lasers with different gain and absorber configurations. Laser Physics. 2020;30, 085003.